Robustness analysis of beamforming based designs for mmWave Full-Duplex Amplify-and-Forward relays

Roberto López-Valcarce, Marcos Martínez-Cotelo
atlanTTic Research Center, University of Vigo, Spain
{valcarce,mmcotelo}@gts.uvigo.es

***Abstract*—We consider the robust design of a millimeter wave MIMO two-hop system in which source, relay and destination are equipped with large antenna arrays. The relay implements the amplify-and-forward protocol and operates in full-duplex mode, thus being subjected to self-interference (SI). Imperfect channel state information (CSI) is assumed in all involved links, including the SI channel, with a deterministic isotropic bounded model on CSI errors. The proposed robust design seeks to maximize the worst-case spectral efficiency, accommodates both digital and phase shifter-based analog beamforming, and is computationally simple; moreover, it does not require knowledge of the size of the CSI uncertainty regions.**

***Index Terms*—Amplify-and-forward relay, millimeter wave communication, robust beamforming, full-duplex.**

I. Introduction

Relaying in general, and Amplify-and-Forward (A&F) relaying in particular, is an appealing way to extend wireless coverage and improve link reliability with low complexity [1], [2]. In Half-Duplex (HD) mode, the relay transmits and receives either in different frequency channels or different time slots, whereas in Full-Duplex (FD) transmission and reception occur simultanously in the same channel. FD relaying has the potential to improve spectral efficiency, although this requires careful management of self-interference (SI) [3], [4]. SI cancellation is usually applied first in the RF analog domain to avoid frontend/ADC saturation, together with a second cancellation stage in the baseband digital domain. With multiple-input multiple-output (MIMO) systems, analog SI cancellation scales poorly in terms of complexity, making *spatial SI suppression* appealing for FD MIMO relays [5], [6], especially at millimeter wave (mmWave) frequencies, for which large antenna arrays are used to overcome the severe path losses [7], [8]. For such large arrays, using an RF chain per antenna is infeasible due to cost and power consumption constraints, and alternative architectures are preferred, e.g., beamforming by means of analog phase shift networks [8], [9]. The ensuing constraints make beamformer design challenging for spatial SI suppression-based FD MIMO [11].

Work supported in part by Agencia Estatal de Investigación (Spain), in part by the European Regional Development Fund (ERDF) through projects TEC2016-76409-C2-2-R, PID2019-105717RB-C21, and in part by Xunta de Galicia (Agrupación Estratéxica Consolidada de Galicia accreditation 2020-2023).

Most previous designs for FD MIMO relays [5], [6], [12], [13] assume perfect channel state information (CSI), with a few exceptions. Under a Decode-and-Forward (D&F) protocol, [14] considers imperfect CSI in all involved links, assumes deterministic ellipsoidal uncertainty regions for the channel errors, and seeks a worst-case optimization design. In [15], imperfect CSI is considered only in the A&F relay-destination (R→D) link, also under a deterministic (isotropic) uncertainty model. Both [14], [15] assume digital beamforming, whereas [16] considers a robust A&F FD relay design under a hybrid digital-analog architecture, with a probabilistic CSI error model for the R→D link. These robust designs result in optimization problems with significant complexity.

We focus on the robust design of A&F FD MIMO relays using digital or analog beamforming. Diferently from [14], [15], [16], which consider multiple single-antenna users, in our setting the destination is a single multiantenna node as in [13]. We adopt a deterministic isotropic CSI error model for all links and maximize the worst-case spectral efficiency of the network. The resulting design has low complexity and does not require explicit knowledge of the size of the uncertainty regions. Simulation results show that the robust FD designs outperform their HD counterparts even in the presence of significant CSI errors.

II. Signal Model

Consider the mmWave network in Fig. 1, comprising nodes S (source), R (relay), and D (destination). Using an array of N_{S} antennas, S sends a data stream to R, which is equipped with receive and transmit arrays of respective sizes N_{R} and N_{T}, whereas D uses a receive array of size N_{D}. It is assumed that the S→D link is absent, and that channels are frequency-flat. The matrices for the S→R and R→D links are $\boldsymbol{H}_{\mathrm{SR}} \in \mathbb{C}^{N_{\mathrm{R}} \times N_{\mathrm{S}}}$ and $\boldsymbol{H}_{\mathrm{RD}} \in \mathbb{C}^{N_{\mathrm{D}} \times N_{\mathrm{T}}}$, respectively. The SI channel is present in FD mode, and is denoted by $\boldsymbol{H}_{\mathrm{RR}} \in \mathbb{C}^{N_{\mathrm{R}} \times N_{\mathrm{T}}}$. The designs considered are model-independent; specific channel models will be presented in Sec. V.

The beamforming vector applied by S is $\boldsymbol{f} \in \mathbb{C}^{N_{\mathrm{S}}}$, whereas $\boldsymbol{v} \in \mathbb{C}^{N_{\mathrm{D}}}$ is the combiner applied by D. Similarly, $\boldsymbol{w} \in \mathbb{C}^{N_{\mathrm{R}}}$ and $\boldsymbol{b} \in \mathbb{C}^{N_{\mathrm{T}}}$ denote the corresponding beamformers at R. The entries of $\boldsymbol{f}$, $\boldsymbol{w}$, $\boldsymbol{b}$ and $\boldsymbol{v}$ have constant magnitude when phase-shifter based analog beamforming is considered. The

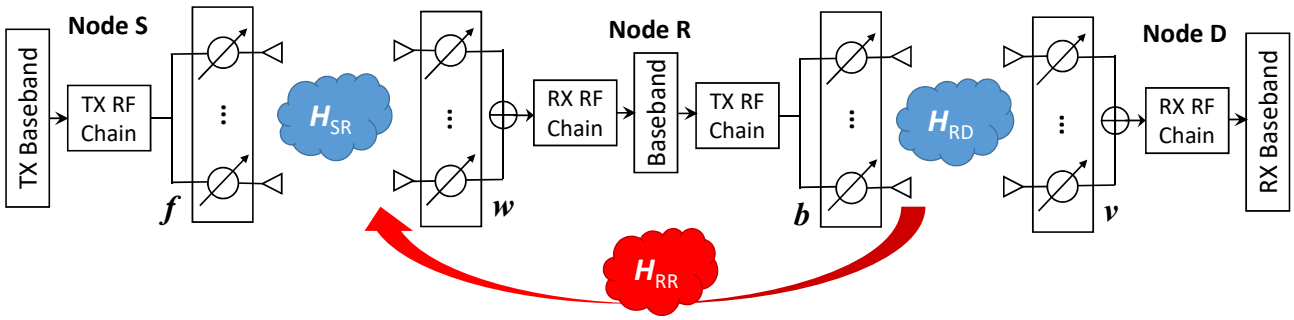

Fig. 1: Analog beamforming-based FD relay network. With digital beamforming, a dedicated RF chain is present at each antenna of every node.

noise vectors $\boldsymbol{n}_{\rm R}$, $\boldsymbol{n}_{\rm D}$ at R and D are zero-mean Gaussian with respective covariance $\sigma_{\rm R}^2\boldsymbol{I}_{N_{\rm R}}$ and $\sigma_{\rm D}^2\boldsymbol{I}_{N_{\rm D}}$, and the average transmit power at S is $\rho_{\rm S}$.

With s the symbol sent from S, the received signal at R is

$$y_{\rm R} = \boldsymbol{w}^H(\sqrt{\rho_{\rm S}}\boldsymbol{H}_{\rm SR}\boldsymbol{f}s + \sqrt{\rho_{\rm SI}}\boldsymbol{H}_{\rm RR}\boldsymbol{b}z + \boldsymbol{n}_{\rm R}), \quad (1)$$

where z is the SI affecting R and $\rho_{\rm SI}$ quantifies SI strength, as both s and z have unit variance. Due to hardware imperfections and processing delay at R, z is a distorted and delayed replica of the signal transmitted by R, plus transmit noise. Note that z is to be understood as residual SI left over by any passive and/or active SI cancellation stages.

Under the A&F protocol, R amplifies its received signal $y_{\rm R}$ and then retransmits it. Thus, the signal at D is given by

$$y_{\rm D} = \boldsymbol{v}^H(\sqrt{g}\boldsymbol{H}_{\rm RD}\boldsymbol{b}y_{\rm R} + \boldsymbol{n}_{\rm D}), \quad (2)$$

with g the power gain of R. Denoting by $\rho_{\rm R}$ the available transmit power at R, it must hold that $g\mathbb{E}\{|y_{\rm R}|^2\} \le \rho_{\rm R}$. We will assume w.l.o.g. that all beamformers $\boldsymbol{f}$, $\boldsymbol{w}$, $\boldsymbol{b}$, $\boldsymbol{v}$ have unit norm, and that the network has channel estimates $\hat{\boldsymbol{H}}_{\rm SR}$, $\hat{\boldsymbol{H}}_{\rm RD}$, $\hat{\boldsymbol{H}}_{\rm RR}$. Denoting the corresponding estimation errors as $\boldsymbol{\Delta}_{\rm SR}$, $\boldsymbol{\Delta}_{\rm RD}$, $\boldsymbol{\Delta}_{\rm RR}$, the true channel matrices are then given by $\boldsymbol{H}_* = \hat{\boldsymbol{H}}_* + \boldsymbol{\Delta}_*$, where '$*$' stands for SR, RD or RR. Define the power gains of the different channels as

$$\begin{aligned} h_{\rm SR}^2(\boldsymbol{w},\boldsymbol{f}) &\triangleq |\boldsymbol{w}^H\boldsymbol{H}_{\rm SR}\boldsymbol{f}|^2 \\ &= |\boldsymbol{w}^H(\hat{\boldsymbol{H}}_{\rm SR}+\boldsymbol{\Delta}_{\rm SR})\boldsymbol{f}|^2, \quad (3) \\ h_{\rm RD}^2(\boldsymbol{v},\boldsymbol{b}) &\triangleq |\boldsymbol{v}^H\boldsymbol{H}_{\rm RD}\boldsymbol{b}|^2 \\ &= |\boldsymbol{v}^H(\hat{\boldsymbol{H}}_{\rm RD}+\boldsymbol{\Delta}_{\rm RD})\boldsymbol{b}|^2, \quad (4) \\ h_{\rm RR}^2(\boldsymbol{w},\boldsymbol{b}) &\triangleq |\boldsymbol{w}^H\boldsymbol{H}_{\rm RR}\boldsymbol{b}|^2 \\ &= |\boldsymbol{w}^H(\hat{\boldsymbol{H}}_{\rm RR}+\boldsymbol{\Delta}_{\rm RR})\boldsymbol{b}|^2, \quad (5) \end{aligned}$$

which will be simply denoted as $h_{\rm SR}^2$, $h_{\rm RD}^2$, $h_{\rm RR}^2$ for brevity. In addition, let us introduce the variables

$$\epsilon_{\rm R} \triangleq \frac{\rho_{\rm S}}{\sigma_{\rm R}^2}, \quad \epsilon_{\rm D} \triangleq \frac{\rho_{\rm R}}{\sigma_{\rm D}^2}, \quad \epsilon_{\rm SI} \triangleq \frac{\rho_{\rm SI}}{\rho_{\rm S}}, \quad q \triangleq \frac{\sigma_{\rm R}^2}{\sigma_{\rm D}^2}g. \quad (6)$$

Assuming Gaussian codebooks and treating SI as noise, the achievable rate (in bits/s/Hz) of this network is found [13]:

$$\mathcal{R}_{\rm FD} = \log_2\left(1 + \frac{q\epsilon_{\rm R}h_{\rm SR}^2h_{\rm RD}^2}{1+qh_{\rm RD}^2(1+\epsilon_{\rm R}\epsilon_{\rm SI}h_{\rm RR}^2)}\right), \quad (7)$$

whereas the relay power constraint can be written as

$$q(1+\epsilon_{\rm R}\epsilon_{\rm SI}h_{\rm RR}^2 + \epsilon_{\rm R}h_{\rm SR}^2) \le \epsilon_{\rm D}. \quad (8)$$

III. Robust Design

We consider a robust design against the worst-case channel estimation errors, under the relay power constraint and appropriate beamformer constraints: in a digital design, each of the vectors $\boldsymbol{f}$, $\boldsymbol{w}$, $\boldsymbol{b}$, $\boldsymbol{v}$ is constrained to be unit-norm (UN), whereas in a phase shifter-based analog design they are constrained to be unit-norm with constant amplitude (UNCA).

Since $\mathcal{R}_{\rm FD}$ in (7) is a monotonically increasing function of q, the optimum strategy is for the relay to transmit at full power, so that equality holds in (8). This can be achieved in practice even in the presence of channel estimation errors by using an automatic gain control (AGC) loop at the relay. Substituting this optimum value of q in (7), we obtain

$$\mathcal{R}_{\rm FD} = \log_2\left(1 + \frac{\epsilon_{\rm R}h_{\rm SR}^2\cdot\epsilon_{\rm D}h_{\rm RD}^2}{(1+\epsilon_{\rm R}\epsilon_{\rm SI}h_{\rm RR}^2)(1+\epsilon_{\rm D}h_{\rm RD}^2)+\epsilon_{\rm R}h_{\rm SR}^2}\right). \quad (9)$$

The robust design is then formulated as

$$\max_{\{\boldsymbol{f},\boldsymbol{w},\boldsymbol{b},\boldsymbol{v}\}} \ \min_{\{\boldsymbol{\Delta}_{\rm SR},\boldsymbol{\Delta}_{\rm RD},\boldsymbol{\Delta}_{\rm RR}\}} \mathcal{R}_{\rm FD}, \quad (10)$$

where the beamformers are constrained to be either UN (digital case) or UNCA (analog case), and in addition we impose the following isotropic uncertainty bounds, as in, e.g., [15]:

$$\|\boldsymbol{\Delta}_{\rm SR}\|_F \le \mu_{\rm R}, \ \ \|\boldsymbol{\Delta}_{\rm RD}\|_F \le \mu_{\rm D}, \ \ \|\boldsymbol{\Delta}_{\rm RR}\|_F \le \mu_{\rm SI}. \quad (11)$$

The constants $\mu_{\rm R}$, $\mu_{\rm D}$, $\mu_{\rm SI}$ reflect our confidence in the quality of the channel estimates; note that without the constraints (11), the worst-case rate would equal zero. The inner minimization in (10) is solved with the aid of the following result, whose proof can be found in Appendix A.

Theorem 1: Given $z \in \mathbb{C}$ and vectors $\boldsymbol{x} \in \mathbb{C}^n$, $\boldsymbol{y} \in \mathbb{C}^m$, let $h(\boldsymbol{\Delta}) = |z + \boldsymbol{x}^H\boldsymbol{\Delta}\boldsymbol{y}|$, for $\boldsymbol{\Delta} \in \mathbb{C}^{n\times m}$. Then, for any $\mu \ge 0$,

$$\begin{aligned} \max_{\|\boldsymbol{\Delta}\|_F\le\mu} h(\boldsymbol{\Delta}) &= |z| + \mu\|\boldsymbol{x}\|_2\|\boldsymbol{y}\|_2, \quad (12) \\ \min_{\|\boldsymbol{\Delta}\|_F\le\mu} h(\boldsymbol{\Delta}) &= \max\{0, |z| - \mu\|\boldsymbol{x}\|_2\|\boldsymbol{y}\|_2\}. \quad (13) \end{aligned}$$

Note that $\mathcal{R}_{\rm FD}$ in (9) is *decreasing* in $h_{\rm RR}^2$, hence minimizing $\mathcal{R}_{\rm FD}$ w.r.t. $\boldsymbol{\Delta}_{\rm RR}$ subject to $\|\boldsymbol{\Delta}_{\rm RR}\|_F \le \mu_{\rm SI}$ amounts to

maximizing $h_{\rm RR}^2 = |\boldsymbol{w}^H \hat{\boldsymbol{H}}_{\rm RR}\boldsymbol{b} + \boldsymbol{w}^H \boldsymbol{\Delta}_{\rm RR}\boldsymbol{b}|^2$ under the same constraint; by Th. 1, the maximum is $h_{\rm RR}^2 = (|\boldsymbol{w}^H \hat{\boldsymbol{H}}_{\rm RR}\boldsymbol{b}| + \mu_{\rm SI}\|\boldsymbol{w}\|_2\|\boldsymbol{b}\|_2)^2$. On the other hand, $\mathcal{R}_{\rm FD}$ in (9) is *increasing* in $h_{\rm SR}^2$, $h_{\rm RD}^2$. By Th. 1, and since under either the UN or UNCA constraints the beamformers have unit norm, the minimum $\mathcal{R}_{\rm FD}$ is obtained when

$$h_{\rm SR} = \bar{h}_{\rm SR} \triangleq \max\{0, |\boldsymbol{w}^H \hat{\boldsymbol{H}}_{\rm SR}\boldsymbol{f}| - \mu_{\rm R}\}, \quad (14)$$

$$h_{\rm RD} = \bar{h}_{\rm RD} \triangleq \max\{0, |\boldsymbol{v}^H \hat{\boldsymbol{H}}_{\rm RD}\boldsymbol{b}| - \mu_{\rm D}\}. \quad (15)$$

Note that if either $h_{\rm SR} = 0$ or $h_{\rm RD} = 0$, then the solution of the inner minimization in (10) is zero, regardless of the beamforming vectors, in which case the worst-case robust design problem ceases to be of use. This is due to the fact that if the magnitude of the channel estimation errors is allowed to be sufficiently large, then it is always possible to find a particular instance of such CSI errors resulting in zero spectral efficiency. To avoid this situation, we need to assume that the zero solution is not attained in (14)-(15), i.e., that there exist unit-norm $\boldsymbol{f}$, $\boldsymbol{w}$, $\boldsymbol{b}$, $\boldsymbol{v}$ such that $|\boldsymbol{w}^H \hat{\boldsymbol{H}}_{\rm SR}\boldsymbol{f}| - \mu_{\rm R} > 0$ and $|\boldsymbol{v}^H \hat{\boldsymbol{H}}_{\rm RD}\boldsymbol{b}| - \mu_{\rm D} > 0$. This, in turn, is equivalent to the following (see Appendix B):

Assumption 1: Let $\sigma_1(\boldsymbol{A})$ denote the largest singular value of $\boldsymbol{A}$. Then $\mu_{\rm R} < \sigma_1(\hat{\boldsymbol{H}}_{\rm SR})$ and $\mu_{\rm D} < \sigma_1(\hat{\boldsymbol{H}}_{\rm RD})$.

Assumption 1 effectively determines the range of relative error magnitude in the S→R and R→D channel estimates since, in view of (11), it implies that

$$\frac{\|\boldsymbol{\Delta}_{\rm SR}\|_F}{\sigma_1(\hat{\boldsymbol{H}}_{\rm SR})} < 1 \quad \text{and} \quad \frac{\|\boldsymbol{\Delta}_{\rm RD}\|_F}{\sigma_1(\hat{\boldsymbol{H}}_{\rm RD})} < 1. \quad (16)$$

Again, the robust design becomes meaningless unless Assumption 1 is adopted, in which case it reduces to

$$\max_{\boldsymbol{f},\boldsymbol{w},\boldsymbol{b},\boldsymbol{v}} \log_2\left(1 + \frac{\epsilon_{\rm R}\bar{h}_{\rm SR}^2 \cdot \epsilon_{\rm D}\bar{h}_{\rm RD}^2}{(1+\epsilon_{\rm R}\epsilon_{\rm SI}\bar{h}_{\rm RR}^2)(1+\epsilon_{\rm D}\bar{h}_{\rm RD}^2)+\epsilon_{\rm R}\bar{h}_{\rm SR}^2}\right) \quad (17)$$

with $\bar{h}_{\rm SR}$, $\bar{h}_{\rm RD}$ as in (14)-(15), and

$$\bar{h}_{\rm RR} \triangleq |\boldsymbol{w}^H \hat{\boldsymbol{H}}_{\rm RR}\boldsymbol{b}| + \mu_{\rm SI}. \quad (18)$$

Problem (17) does not admit a closed-form solution either under UN or UNCA constraints. However, it can be approached in the same way as in [13] by noting that the objective is monotonically decreasing in $|\boldsymbol{w}^H \hat{\boldsymbol{H}}_{\rm RR}\boldsymbol{b}|$, and increasing in $|\boldsymbol{w}^H \hat{\boldsymbol{H}}_{\rm SR}\boldsymbol{f}|$ and $|\boldsymbol{v}^H \hat{\boldsymbol{H}}_{\rm RD}\boldsymbol{b}|$. The idea is to impose an additional zero-forcing (ZF) constraint $\boldsymbol{w}^H \hat{\boldsymbol{H}}_{\rm RR}\boldsymbol{b} = 0$ on the SI term, as this yields the minimum value of $\bar{h}_{\rm RR}^2 = \mu_{\rm SI}^2$. Then the terms $\bar{h}_{\rm SR}^2$ and $\bar{h}_{\rm RD}^2$ are maximized cyclically subject to the ZF constraint and the appropriate constraints (UN or UNCA) on beamformers. Maximizing $\bar{h}_{\rm SR}^2$ (resp. $\bar{h}_{\rm RD}^2$) amounts to maximizing $|\boldsymbol{w}^H \hat{\boldsymbol{H}}_{\rm SR}\boldsymbol{f}|$ (resp. $|\boldsymbol{v}^H \hat{\boldsymbol{H}}_{\rm RD}\boldsymbol{b}|$). Thus, the low-complexity UN/UNCA beamformer designs from [13] can be directly applied in this setting, with the analysis above showing their robustness in that they seek to maximize a worst-case lower bound to spectral efficiency. Note that, apart for Assumption 1, no knowledge about the specific values of $\mu_{\rm R}$, $\mu_{\rm D}$, $\mu_{\rm SI}$ is explicitly needed in this approach.

IV. Half-Duplex case

For completeness, and in order to provide a meaningful benchmark, we consider the HD mode, for which $\rho_{\rm SI} = 0$ in (1). If the available bandwidth is split in half between the S→R and R→D links, then for the same noise psd as in FD the corresponding noise powers become $\frac{\sigma_{\rm R}^2}{2}$ and $\frac{\sigma_{\rm D}^2}{2}$. If orthogonal time slots of equal duration are used instead, then for the same energy per symbol as in FD the corresponding transmission powers become $2\rho_{\rm S}$ and $2\rho_{\rm R}$. In either case, the SNR values $\epsilon_{\rm R}$, $\epsilon_{\rm D}$ become $2\epsilon_{\rm R}$ and $2\epsilon_{\rm R}$. Taking also into account that (i) the transmission of a symbol takes now two channel uses, (ii) the ratio $\frac{\sigma_{\rm R}^2}{\sigma_{\rm D}^2}$ (hence the scaled gain q) remains the same, and (iii) $\epsilon_{\rm SI} = 0$, the achievable rate and power constraint of the HD relay network become

$$\mathcal{R}_{\rm HD} = \frac{1}{2}\log_2\left(1 + \frac{2q\epsilon_{\rm R}h_{\rm SR}^2 h_{\rm RD}^2}{1 + qh_{\rm RD}^2}\right), \; q(1 + 2\epsilon_{\rm R}h_{\rm SR}^2) \le 2\epsilon_{\rm D}, \quad (19)$$

with $h_{\rm SR}^2$, $h_{\rm RD}^2$ given by (3)-(4). Since $\mathcal{R}_{\rm HD}$ is maximized w.r.t. q for full power transmission, the robust design becomes

$$\max_{\boldsymbol{f},\boldsymbol{w},\boldsymbol{b},\boldsymbol{v}} \min_{\boldsymbol{\Delta}_{\rm SR},\boldsymbol{\Delta}_{\rm RD}} \frac{1}{2}\log_2\left(1 + \frac{2\epsilon_{\rm R}h_{\rm SR}^2 \cdot 2\epsilon_{\rm D}h_{\rm RD}^2}{1 + 2\epsilon_{\rm R}h_{\rm SR}^2 + 2\epsilon_{\rm D}h_{\rm RD}^2}\right), \quad (20)$$

under UN/UNCA constraints on beamformers and constraints (11) on error matrices. Following steps analogous to those in Sec. III, under Assumption 1 problem (20) reduces to

$$\max_{\boldsymbol{f},\boldsymbol{w},\boldsymbol{b},\boldsymbol{v}} \frac{1}{2}\log_2\left(1 + \frac{2\epsilon_{\rm R}\bar{h}_{\rm SR}^2 \cdot 2\epsilon_{\rm D}\bar{h}_{\rm RD}^2}{1 + 2\epsilon_{\rm R}\bar{h}_{\rm SR}^2 + 2\epsilon_{\rm D}\bar{h}_{\rm RD}^2}\right), \quad (21)$$

with $\bar{h}_{\rm SR}^2$ and $\bar{h}_{\rm RD}^2$ as in (14)-(15). There is no coupling between S→R and R→D variables now, so (21) amounts to

$$\max_{\boldsymbol{f},\boldsymbol{w}} |\boldsymbol{w}^H \hat{\boldsymbol{H}}_{\rm SR}\boldsymbol{f}|, \qquad \max_{\boldsymbol{b},\boldsymbol{v}} |\boldsymbol{v}^H \hat{\boldsymbol{H}}_{\rm RD}\boldsymbol{b}|. \quad (22)$$

Under UN constraints, the solution is the largest singular value of $\hat{\boldsymbol{H}}_{\rm SR}$ and $\hat{\boldsymbol{H}}_{\rm RD}$, respectively. Under UNCA constraints, there is no closed-form solution to (22). Nevertheless, if either $\boldsymbol{w}$ or $\boldsymbol{f}$ is held fixed, then $|\boldsymbol{w}^H \hat{\boldsymbol{H}}_{\rm SR}\boldsymbol{f}|$ can be maximized in closed form in terms of the other, so that a cyclic maximization approach seems natural; and similarly for $|\boldsymbol{v}^H \hat{\boldsymbol{H}}_{\rm RD}\boldsymbol{b}|$. Again, knowledge of $\mu_{\rm R}$, $\mu_{\rm D}$ is not required.

V. Results

The S, R and D nodes are equipped with 16-antenna $\frac{\lambda}{2}$-spaced uniform linear arrays. For the S→R and R→D channels, the Saleh-Valenzuela narrowband clustered model [17] is assumed, with $N_{\rm cl}$ scattering clusters and $N_{\rm ray}$ rays per cluster:

$$\boldsymbol{H}_{\rm SR/RD} = \sum_{k=1}^{N_{\rm cl}} \sum_{\ell=1}^{N_{\rm ray}} \beta_{k,\ell}\boldsymbol{a}_{\rm r}(\varphi_{k,\ell})\boldsymbol{a}_{\rm t}^H(\theta_{k,\ell}), \quad (23)$$

where for the ℓ-th ray in the k-th cluster, $\boldsymbol{a}_{\rm t}(\theta_{k,\ell})$ and $\boldsymbol{a}_{\rm r}(\varphi_{k,\ell})$ are the antenna array steering and response vectors at the transmitter and receiver, respectively, evaluated at the corresponding azimuth angles of departure from transmitter, $\theta_{k,\ell}$, or arrival at receiver, $\varphi_{k,\ell}$; and $\beta_{k,\ell}$ is the complex gain.

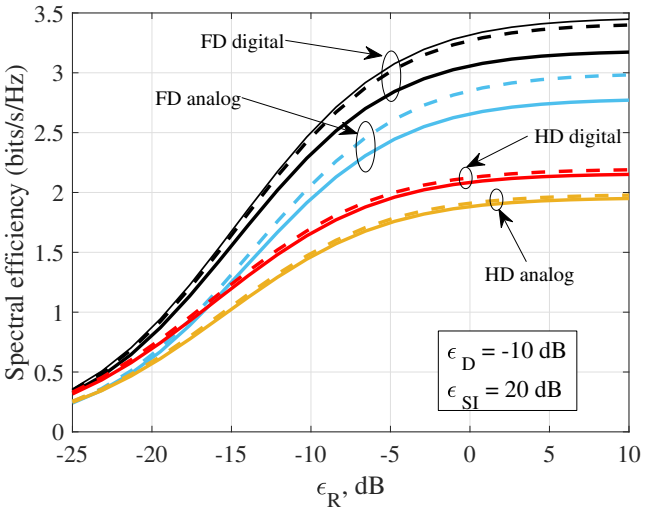

Fig. 2: Spectral efficiency vs. SNR at R. Dashed: perfect CSI. Solid: imperfect CSI ($\sigma_\gamma = 0.3$, $\sigma_\phi = 10°$). Thin solid: FD digital upper bound (no SI and perfect CSI).

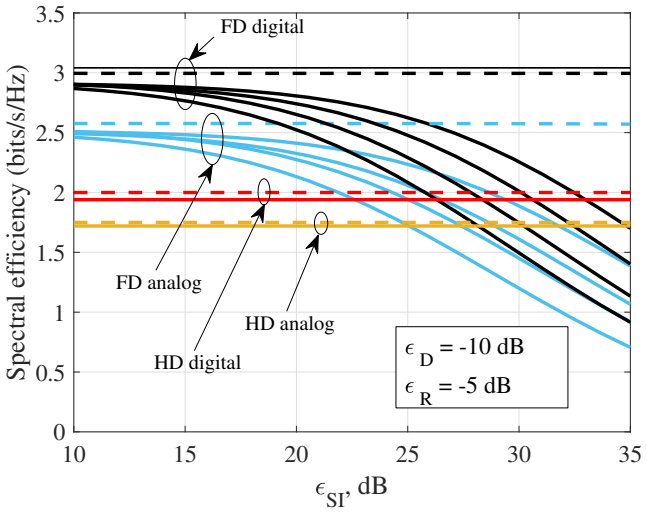

Fig. 3: Spectral efficiency vs. SI strength. Dashed: perfect CSI. Solid: imperfect CSI. Thin solid: FD digital bound.

The SI channel has a near-field line-of-sight (LOS) component, and a far-field one due to SI reflections in nearby scatterers:

$$\boldsymbol{H}_{\mathrm{RR}} = \sqrt{\frac{\kappa}{\kappa+1}}\boldsymbol{H}_{\mathrm{LOS}} + \sqrt{\frac{1}{\kappa+1}}\boldsymbol{H}_{\mathrm{REF}}, \qquad (24)$$

with κ the Rice factor. For the far-field term $\boldsymbol{H}_{\mathrm{REF}}$ the same model as in (23) is adopted, whereas the LOS component follows the near-field model [10], [11]

$$[\boldsymbol{H}_{\mathrm{LOS}}]_{pq} = \frac{1}{d_{pq}} e^{-j2\pi\frac{d_{pq}}{\lambda}}, \qquad (25)$$

with d_{pq} the distance from the p-th antenna of the TX array to the q-th antenna of the RX array, and λ the wavelength. For the arrays at R the geometry of [11, Fig. 2] is assumed, with distance $d = 2\lambda$ and angle $\omega = \frac{\pi}{2}$.

We assumed $N_{\mathrm{cl}} = 6$, $N_{\mathrm{ray}} = 10$ and $\kappa = 10$ dB. Such relatively large value of the Rice factor is realistic, given the proximity between the TX and RX arrays at the relay. Departure/arrival angles are random, with mean cluster angle uniformly distributed in $[0, 360°]$ and angular spreads of $16°$. Path gains are i.i.d. complex circular Gaussian with the same variance. Channel matrices are normalized so that their squared Frobenius norms equal the number of their entries. For a given $\boldsymbol{H}$, CSI errors are introduced entrywise as $[\hat{\boldsymbol{H}}]_{pq} = [\boldsymbol{H}]_{pq}(1+\gamma_{pq})e^{j\phi_{pq}}$, with γ_{pq} and ϕ_{pq} independent zero-mean Gaussian random variables with variances σ_γ^2 and σ_ϕ^2, respectively. Regarding the SI channel, we assume that its LOS component $\boldsymbol{H}_{\mathrm{LOS}}$ can be accurately obtained in an initial calibration stage, whereas the far-field component $\boldsymbol{H}_{\mathrm{REF}}$ is subject to estimation errors as above.

The spectral efficiency was computed by averaging over 500 channel realizations. First we fixed the SNR at D as $\epsilon_{\mathrm{D}} = -10$ dB, and with a rather large self-interference to signal ratio at the relay of $\epsilon_{\mathrm{SI}} = 20$ dB. CSI errors were generated with $\sigma_\gamma = 0.3$, $\sigma_\phi = 10°$ for $\boldsymbol{H}_{\mathrm{SR}}$, $\boldsymbol{H}_{\mathrm{RD}}$ and $\boldsymbol{H}_{\mathrm{REF}}$. Fig. 2 shows that the FD relay is more sensitive than the HD designs, due mainly to incomplete SI cancellation due to errors in the SI channel estimate. Nevertheless, even with these relatively large CSI errors and SI strength, the degradation is not too severe.

Next we fixed $\epsilon_{\mathrm{D}} = -10$ dB and $\epsilon_{\mathrm{R}} = -5$ dB. For $\boldsymbol{H}_{\mathrm{SR}}$ and $\boldsymbol{H}_{\mathrm{RD}}$, CSI errors were generated with $\sigma_\gamma = 0.3$, $\sigma_\phi = 10°$ as before; whereas for $\boldsymbol{H}_{\mathrm{REF}}$, we took $\sigma_\gamma = 0.3$ and swept over $\sigma_\phi \in \{10°, 20°, 30°, 40°\}$ to check the effect of incomplete SI cancellation in the FD designs. Although the importance of accurate estimation of the SI channel is clear, Fig. 3 shows that performance degradation is graceful, as expected from the robustness analysis of Sec. III. Even for values as large as $\sigma_\phi = 40°$, the digital and analog FD designs still outperform their corresponding HD counterparts for values of ϵ_{SI} up to 26 and 25 dB, respectively. Imperfect CSI in the S→R and R→D links seems to be much less detrimental in comparison. This is further illustrated in Fig. 4, which shows the degradation of the spectral efficiency for each design under four different settings: (a) perfect CSI in all links; (b) CSI errors in the S→R link only; (c) CSI errors in the R→D link only; (d) CSI errors in the far-field term of the SI channel only. CSI errors were generated with $\sigma_\gamma = 0.3$ and varying σ_ϕ. The larger sensitivity to CSI errors in the SI channel of the FD designs is clear; errors in the R→D link have a larger impact than those in the S→R link because the latter has a larger SNR.

VI. Conclusion

The HD/FD digital/analog beamforming designs discussed are inherently robust to CSI errors; moreover, they have low complexity and do not require knowledge of the sizes of uncertainty regions, which is a very appealing feature in practice. In particular, FD designs still outperform their HD counterparts even in the presence of significant CSI errors. Future work will address extensions to nonisotropic error

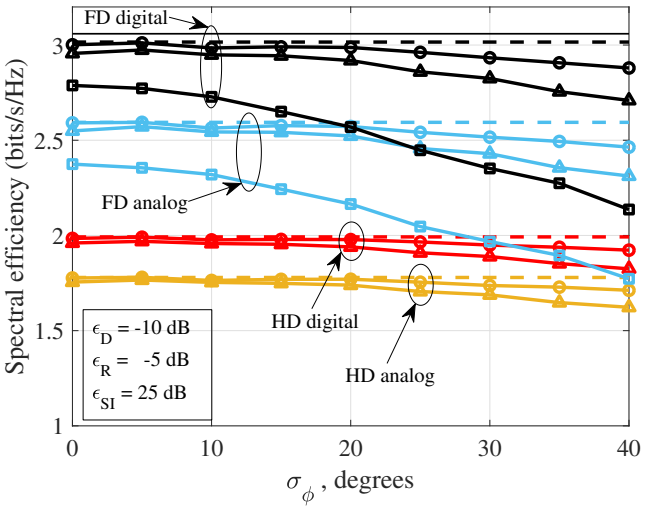

Fig. 4: Spectral efficiency vs. CSI errors. Dashed: perfect CSI. Thin solid: FD digital bound. Errors in S→R link (○), R→D link (△), Self-Interference channel (□).

models, as well as to hybrid analog/digital architectures with finite-resolution phase shifters, handling multiple data streams.

APPENDIX

A. Proof of Theorem 1

Using the triangle inequality,

$$h(\boldsymbol{\Delta}) \leq |z| + \sum_{i=1}^{n}\sum_{j=1}^{m} |x_i||y_j||\Delta_{ij}|. \tag{26}$$

At the maximum of the right-hand side of (26) subject to $\|\boldsymbol{\Delta}\|_F^2 = \sum_{i=1}^{n}\sum_{j=1}^{m}|\Delta_{ij}|^2 \leq \mu^2$, the constraint must hold with equality. Using Lagrange multipliers, such maximum is found to take place at

$$|\Delta_{ij}| = \mu \frac{|x_i|}{\|\boldsymbol{x}\|_2}\frac{|y_j|}{\|\boldsymbol{y}\|_2}, \quad i = 1,\ldots,n, \;\; j = 1,\ldots,m, \tag{27}$$

hence (26) yields $h(\boldsymbol{\Delta}) \leq |z| + \mu\|\boldsymbol{x}\|_2\|\boldsymbol{y}\|_2$; the bound is achieved by

$$\boldsymbol{\Delta} = \frac{\boldsymbol{x}}{\|\boldsymbol{x}\|_2}\frac{\boldsymbol{y}^H}{\|\boldsymbol{y}\|_2}\mu e^{j\angle z}, \tag{28}$$

which proves the first part of the theorem. To prove the second part, assume first that $|z| \leq \mu\|\boldsymbol{x}\|_2\|\boldsymbol{y}\|_2$. Then $\boldsymbol{\Delta} = -z\frac{\boldsymbol{x}}{\|\boldsymbol{x}\|_2^2}\frac{\boldsymbol{y}^H}{\|\boldsymbol{y}\|_2^2}$ is feasible and yields $h(\boldsymbol{\Delta}) = 0$, which is clearly minimum.

Assume then $|z| \geq \mu\|\boldsymbol{x}\|_2\|\boldsymbol{y}\|_2$. As seen above, for all $\boldsymbol{\Delta}$ for which $\|\boldsymbol{\Delta}\|_F \leq \mu$, it holds that $|\boldsymbol{x}^H\boldsymbol{\Delta}\boldsymbol{y}| \leq \mu\|\boldsymbol{x}\|_2\|\boldsymbol{y}\|_2$, and thus $|z| - |\boldsymbol{x}^H\boldsymbol{\Delta}\boldsymbol{y}| \geq 0$. By the triangle inequality,

$$\begin{aligned} h(\boldsymbol{\Delta}) &\geq \big||z| - |\boldsymbol{x}^H\boldsymbol{\Delta}\boldsymbol{y}|\big| = |z| - |\boldsymbol{x}^H\boldsymbol{\Delta}\boldsymbol{y}| \\ &\geq |z| - \mu\|\boldsymbol{x}\|_2\|\boldsymbol{y}\|_2, \end{aligned} \tag{29}$$

and the bound is achieved by

$$\boldsymbol{\Delta} = -\frac{\boldsymbol{x}}{\|\boldsymbol{x}\|_2}\frac{\boldsymbol{y}^H}{\|\boldsymbol{y}\|_2}\mu e^{j\angle z}. \tag{30}$$

B. On Assumption 1

Given a matrix $\boldsymbol{H}$ and a constant $\mu > 0$, we shall show the equivalence of the following statements:

1) There exist unit-norm vectors $\boldsymbol{x}$, $\boldsymbol{y}$ such that $|\boldsymbol{x}^H\boldsymbol{H}\boldsymbol{y}| - \mu > 0$.
2) $\mu < \sigma_1(\boldsymbol{H})$.

Assume 1) is true. Since

$$\sigma_1(\boldsymbol{H}) = \max_{\|\boldsymbol{u}\|_2=1,\|\boldsymbol{v}\|_2=1} |\boldsymbol{u}^H\boldsymbol{H}\boldsymbol{v}|, \tag{31}$$

it follows that

$$\mu < |\boldsymbol{x}^H\boldsymbol{H}\boldsymbol{y}| \leq \sigma_1(\boldsymbol{H}). \tag{32}$$

Now assume 2) is true. Let $\boldsymbol{x}$, $\boldsymbol{y}$ be the (unit-norm) principal left and right singular vectors of $\boldsymbol{H}$, respectively. Then $|\boldsymbol{x}^H\boldsymbol{H}\boldsymbol{y}| = \sigma_1(\boldsymbol{H}) > \mu$, so that $|\boldsymbol{x}^H\boldsymbol{H}\boldsymbol{y}| - \mu > 0$. Therefore both statements are equivalent.

REFERENCES

[1] D. Soldani and S. Dixit, "Wireless relays for broadband access," *IEEE Commun. Mag.,* vol. 46, no. 3, pp. 58–66, Mar. 2008.

[2] L. Jimenez Rodriguez, N. Tran and T. Le-Ngoc, *Amplify-and-Forward Relaying in Wireless Communications.* Springer, 2015.

[3] M. Heino *et al.,* "Recent advances in antenna design and interference cancellation algorithms for in-band full-duplex relays," *IEEE Commun. Mag.,* vol. 53, no. 5, pp. 91–101, May 2015.

[4] Z. Zhang, K. Long, A. V. Vasilakos and L. Hanzo, "Full-duplex wireless communications: Challenges, solutions, and future research directions," *Proc. IEEE,* vol. 104, no. 7, pp. 1369–1409, Jul. 2016.

[5] T. Riihonen, S. Werner and R. Wichman, "Mitigation of loopback self-interference in full-duplex MIMO relays," *IEEE Trans. Signal Process.,* vol. 59, no. 12, pp. 5983–5993, Dec. 2011.

[6] B. Day, A. Margetts, D. Bliss and P. Schniter, "Full-duplex MIMO relaying: Achievable rates under limited dynamic range," *IEEE J. Sel. Areas Commun.,* vol. 30, no. 8, pp. 1541–1553, Sep. 2012.

[7] Z. Pi and F. Khan, "An introduction to mmWave mobile broadband systems," *IEEE Commun. Mag.,* vol. 49, no. 6, pp. 101-107, Jun. 2011.

[8] R. W. Heath Jr., N. González-Prelcic, S. Rangan, W. Roh and A. Sayeed, "An overview of signal processing techniques for millimeter wave MIMO systems," *IEEE J. Sel. Topics Signal Process.,* vol. 10, no. 3, pp. 436–453, Apr. 2016.

[9] V. Venkateswaran and A.-J. van der Veen, "Analog beamforming in MIMO communications with phase shift networks and online channel estimation," *IEEE Trans. Signal Process.,* vol. 58, no. 8, pp. 4131-4143, Aug. 2010.

[10] L. Li, K. Josiam and R. Taori, "Feasibility study of full-duplex wireless millimeter-wave systems," *Proc. IEEE Int. Conf. Acoust., Speech, Signal Process. (ICASSP),* 2014, pp. 2769–2773.

[11] Z. Xiao, P. Xia and X.-G. Xia, "Full-duplex millimeter-wave communication," *IEEE Wireless Commun.,* pp. 136–143, Dec. 2017.

[12] O. Taghizadeh, J. Zhang and M. Haardt, "Transmit beamforming aided amplify-and-forward MIMO full-duplex relaying with limited dynamic range," *Signal Process.,* vol. 127, pp. 266-281, Oct. 2016.

[13] R. López-Valcarce and N. González-Prelcic, "Beamformer design for full-duplex amplify-and-forward millimeter wave relays," *Proc. Int. Symp. Wireless Commun. Syst. (ISWCS),* 2019.

[14] O. Taghizadeh and R. Mathar, "Robust multi-user decode-and-forward relaying with full-duplex operation," *Proc. Int. Symp. Wireless Commun. Syst. (ISWCS),* 2014.

[15] Y. Xu *et al.,* "Robust transceiver design for full-duplex MIMO relay systems," *Proc. IEEE Global Commun. Conf. (GLOBECOM),* 2017.

[16] Y. Cai *et al.,* "Robust hybrid transceiver design for millimeter wave full-duplex MIMO relay systems," *IEEE Trans. Wireless Commun.,* vol 18, no. 2, pp. 1199–1215, Feb. 2019.

[17] O. El Ayach, S. Rajagopal, S. Abu-Surra, Z. Pi, R. W. Heath, Jr., "Spatially sparse precoding in mmWave MIMO systems," *IEEE Trans. Wireless Commun.,* vol. 13, no. 3, pp. 1499–1513, Mar. 2014.